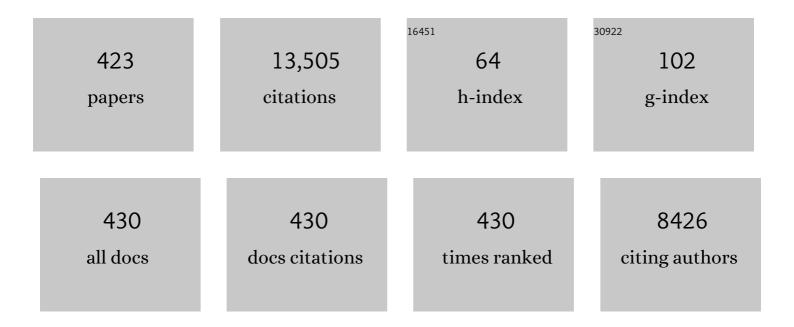
Heang-Ping Chan

List of Publications by Year in descending order

Source: https://exaly.com/author-pdf/1330380/publications.pdf Version: 2024-02-01



#	Article	IF	CITATIONS
1	Effect of Dose Level on Radiologists' Detection of Microcalcifications in Digital Breast Tomosynthesis: An Observer Study with Breast Phantoms. Academic Radiology, 2022, 29, S42-S49.	2.5	3
2	Computerized Decision Support for Bladder Cancer Treatment Response Assessment in CT Urography: Effect on Diagnostic Accuracy in Multi-Institution Multi-Specialty Study. Tomography, 2022, 8, 644-656.	1.8	5
3	Deep convolutional neural network regularized digital breast tomosynthesis reconstruction with detector blur and correlated noise modeling. , 2022, , .		1
4	Recursive Training Strategy for a Deep Learning Network for Segmentation of Pathology Nuclei With Incomplete Annotation. IEEE Access, 2022, 10, 49337-49346.	4.2	2
5	Assessment of taskâ€based performance from five clinical DBT systems using an anthropomorphic breast phantom. Medical Physics, 2021, 48, 1026-1038.	3.0	10
6	Deep Convolutional Neural Network With Adversarial Training for Denoising Digital Breast Tomosynthesis Images. IEEE Transactions on Medical Imaging, 2021, 40, 1805-1816.	8.9	19
7	Image Processing Analytics: Enhancements and Segmentation. , 2021, , 1727-1745.		0
8	Prediction of Disease Free Survival in Laryngeal and Hypopharyngeal Cancers Using CT Perfusion and Radiomic Features: A Pilot Study. Tomography, 2021, 7, 10-19.	1.8	7
9	Risks of feature leakage and sample size dependencies in deep feature extraction for breast mass classification. Medical Physics, 2021, 48, 2827-2837.	3.0	16
10	Promise and Potential Pitfalls: Re-creating Images or Generating New Images for Al Modeling. Radiology: Artificial Intelligence, 2021, 3, e210102.	5.8	1
11	Al in medical physics: guidelines for publication. Medical Physics, 2021, 48, 4711-4714.	3.0	24
12	Using Single-View Wide-Angle DBT with AI for Breast Cancer Screening. Radiology, 2021, 300, 537-538.	7.3	2
13	Quantitative Imaging and Bladder Cancer. , 2021, , 1-32.		0
14	CAD and AI for breast cancer—recent development and challenges. British Journal of Radiology, 2020, 93, 20190580.	2.2	100
15	Digital Breast Tomosynthesis Slab Thickness: Impact on Reader Performance and Interpretation Time. Radiology, 2020, 297, 534-542.	7.3	5
16	Computerâ€aided diagnosis in the era of deep learning. Medical Physics, 2020, 47, e218-e227.	3.0	154
17	Pathologic categorization of lung nodules: Radiomic descriptors of CT attenuation distribution patterns of solid and subsolid nodules in low-dose CT. European Journal of Radiology, 2020, 129, 109106.	2.6	4
18	Generalization error analysis for deep convolutional neural network with transfer learning in breast cancer diagnosis. Physics in Medicine and Biology, 2020, 65, 105002.	3.0	23

#	Article	IF	CITATIONS
19	Deep Learning in Medical Image Analysis. Advances in Experimental Medicine and Biology, 2020, 1213, 3-21.	1.6	300
20	Explainable AI for medical imaging: deep-learning CNN ensemble for classification of estrogen receptor status from breast MRI. , 2020, , .		28
21	Deep convolutional neural network denoising for digital breast tomosynthesis reconstruction. , 2020, , .		7
22	Assessment of task-based performance from five clinical DBT systems using an anthropomorphic breast phantom. , 2020, , .		2
23	Standardization in Quantitative Imaging: A Multicenter Comparison of Radiomic Features from Different Software Packages on Digital Reference Objects and Patient Data Sets. Tomography, 2020, 6, 118-128.	1.8	61
24	Intraobserver Variability in Bladder Cancer Treatment Response Assessment With and Without Computerized Decision Support. Tomography, 2020, 6, 194-202.	1.8	13
25	Hazards of data leakage in machine learning: a study on classification of breast cancer using deep neural networks. , 2020, , .		8
26	Convolutional neural network-based decision support system for bladder cancer staging in CT urography: decision threshold estimation and validation. , 2020, , .		1
27	Hybrid deep-learning model for volume segmentation of lung nodules in CT images. , 2020, , .		Ο
28	Bladder wall segmentation using U-net based deep learning. , 2020, , .		0
29	Generating high resolution digital mammogram from digitized film mammogram with conditional generative adversarial network. , 2020, , .		2
30	Effect of source blur on digital breast tomosynthesis reconstruction. Medical Physics, 2019, 46, 5572-5592.	3.0	10
31	Deep Learning Approach for Assessment of Bladder Cancer Treatment Response. Tomography, 2019, 5, 201-208.	1.8	38
32	Variabilities in Reference Standard by Radiologists and Performance Assessment in Detection of Pulmonary Embolism in CT Pulmonary Angiography. Journal of Digital Imaging, 2019, 32, 1089-1096.	2.9	7
33	Automated pectoral muscle identification on <scp>MLO</scp> â€view mammograms: Comparison of deep neural network to conventional computer vision. Medical Physics, 2019, 46, 2103-2114.	3.0	10
34	Uâ€Net based deep learning bladder segmentation in <scp>CT</scp> urography. Medical Physics, 2019, 46, 1752-1765.	3.0	50
35	Breast Cancer Diagnosis in Digital Breast Tomosynthesis: Effects of Training Sample Size on Multi-Stage Transfer Learning Using Deep Neural Nets. IEEE Transactions on Medical Imaging, 2019, 38, 686-696.	8.9	147
36	Diagnostic Accuracy of CT for Prediction of Bladder Cancer Treatment Response with and without Computerized Decision Support. Academic Radiology, 2019, 26, 1137-1145.	2.5	46

#	Article	IF	CITATIONS
37	Synthesizing mammogram from digital breast tomosynthesis. Physics in Medicine and Biology, 2019, 64, 045011.	3.0	9
38	Deep Learning for Mammographic Breast Density Assessment and Beyond. Radiology, 2019, 290, 59-60.	7.3	9
39	Deepâ€learning convolutional neural network: Inner and outer bladder wall segmentation in CT urography. Medical Physics, 2019, 46, 634-648.	3.0	15
40	Multi-path deep learning model for automated mammographic density categorization. , 2019, , .		3
41	2D and 3D bladder segmentation using U-Net-based deep-learning. , 2019, , .		4
42	Quantitative MRI biomarker for treatment response assessment of multiple myeloma: robustness evaluation using independent test set of prospective cases. , 2019, , .		0
43	Analysis of mammographic density as a predictor for breast cancer occurrence. , 2019, , .		Ο
44	Deep learning based bladder cancer treatment response assessment. , 2019, , .		0
45	Homogenization of breast MRI across imaging centers and feature analysis using unsupervised deep embedding. , 2019, , .		1
46	Analysis of deep convolutional features for detection of lung nodules in computed tomography. , 2019, , .		3
47	Bladder cancer staging in CT urography: estimation and validation of decision thresholds for a radiomics-based decision support system. , 2019, , .		Ο
48	Interrater Agreement and Diagnostic Accuracy of a Novel Computer-Aided Detection Process for the Detection and Prevention of Retained Surgical Instruments. American Journal of Roentgenology, 2018, 210, 709-714.	2.2	2
49	Evolutionary pruning of transfer learned deep convolutional neural network for breast cancer diagnosis in digital breast tomosynthesis. Physics in Medicine and Biology, 2018, 63, 095005.	3.0	74
50	Semiâ€automated pulmonary nodule interval segmentation using the <scp>NLST</scp> data. Medical Physics, 2018, 45, 1093-1107.	3.0	17
51	Detector Blur and Correlated Noise Modeling for Digital Breast Tomosynthesis Reconstruction. IEEE Transactions on Medical Imaging, 2018, 37, 116-127.	8.9	17
52	Computer-aided assessment of breast density: comparison of supervised deep learning and feature-based statistical learning. Physics in Medicine and Biology, 2018, 63, 025005.	3.0	44
53	Assessment of mammographic breast density after sleeve gastrectomy. Surgery for Obesity and Related Diseases, 2018, 14, 1643-1651.	1.2	3
54	Generalization error analysis: deep convolutional neural network in mammography. , 2018, , .		2

#	Article	IF	CITATIONS
55	Compression of deep convolutional neural network for computer-aided diagnosis of masses in digital breast tomosynthesis. , 2018, , .		1
56	Cross-domain and multi-task transfer learning of deep convolutional neural network for breast cancer diagnosis in digital breast tomosynthesis. , 2018, , .		9
57	Differentiating invasive and pre-invasive lung cancer by quantitative analysis of histopathologic images. , 2018, , .		1
58	Bladder cancer treatment response assessment with radiomic, clinical, and radiologist semantic features. , 2018, , .		0
59	Computer-aided detection of bladder wall thickening in CT urography (CTU). , 2018, , .		Ο
60	Bladder cancer treatment response assessment in CT urography using two-channel deep-learning network. , 2018, , .		1
61	Bladder cancer staging in CT urography: effect of stage labels on statistical modeling of a decision support system. , 2018, , .		0
62	Deep convolutional neural network for mammographic density segmentation. , 2018, , .		0
63	Fully automated pectoral muscle identification on MLO-view mammograms with deep convolutional neural network. , 2018, , .		1
64	Segmented separable footprint projector for digital breast tomosynthesis and its application for subpixel reconstruction. Medical Physics, 2017, 44, 986-1001.	3.0	4
65	Bladder cancer treatment response assessment using deep learning in CT with transfer learning. , 2017, , .		1
66	Segmentation of inner and outer bladder wall using deep-learning convolutional neural network in CT urography. Proceedings of SPIE, 2017, , .	0.8	10
67	Effects of detector blur and correlated noise on digital breast tomosynthesis reconstruction. , 2017, , \cdot		2
68	Computerâ€∎ided detection of retained surgical needles from postoperative radiographs. Medical Physics, 2017, 44, 180-191.	3.0	3
69	Radiomic modeling of BI-RADS density categories. Proceedings of SPIE, 2017, , .	0.8	Ο
70	Quantitative analysis of CT attenuation distribution patterns of nodule components for pathologic categorization of lung nodules. Proceedings of SPIE, 2017, , .	0.8	1
71	Radiomics biomarkers for accurate tumor progression prediction of oropharyngeal cancer. Proceedings of SPIE, 2017, , .	0.8	1
72	Multi-task transfer learning deep convolutional neural network: application to computer-aided diagnosis of breast cancer on mammograms. Physics in Medicine and Biology, 2017, 62, 8894-8908.	3.0	151

#	Article	IF	CITATIONS
73	Improving image quality for digital breast tomosynthesis: an automated detection and diffusion-based method for metal artifact reduction. Physics in Medicine and Biology, 2017, 62, 7765-7783.	3.0	7
74	Bladder Cancer Treatment Response Assessment in CT using Radiomics with Deep-Learning. Scientific Reports, 2017, 7, 8738.	3.3	144
75	Urinary bladder cancer staging in <scp>CT</scp> urography using machine learning. Medical Physics, 2017, 44, 5814-5823.	3.0	79
76	Characterization of Breast Masses in Digital Breast Tomosynthesis and Digital Mammograms. Academic Radiology, 2017, 24, 1372-1379.	2.5	22
77	Identifying key radiogenomic associations between DCE-MRI and micro-RNA expressions for breast cancer. , 2017, , .		1
78	Breast Density Following Bariatric Surgery: Is BI-RADS the Answer?. Surgery for Obesity and Related Diseases, 2017, 13, S155-S156.	1.2	0
79	Computer-aided detection of bladder masses in CT urography (CTU). Proceedings of SPIE, 2017, , .	0.8	4
80	Bladder Cancer Segmentation in CT for Treatment Response Assessment: Application of Deep-Learning Convolution Neural Network—A Pilot Study. Tomography, 2016, 2, 421-429.	1.8	64
81	Best-Quality Vessel Identification Using Vessel Quality Measure in Multiple-Phase Coronary CT Angiography. Computational and Mathematical Methods in Medicine, 2016, 2016, 1-13.	1.3	1
82	Computer-aided detection of bladder mass within non-contrast-enhanced region of CT Urography (CTU). Proceedings of SPIE, 2016, , .	0.8	1
83	Automatic detection of ureter lesions in CT urography. , 2016, , .		0
84	Analysis of computer-aided detection techniques and signal characteristics for clustered microcalcifications on digital mammography and digital breast tomosynthesis. Physics in Medicine and Biology, 2016, 61, 7092-7112.	3.0	19
85	Mass detection in digital breast tomosynthesis: Deep convolutional neural network with transfer learning from mammography. Medical Physics, 2016, 43, 6654-6666.	3.0	232
86	Coronary artery analysis: Computerâ€assisted selection of bestâ€quality segments in multipleâ€phase coronary CT angiography. Medical Physics, 2016, 43, 5268-5278.	3.0	2
87	A Similarity Study of Interactive Content-Based Image Retrieval Scheme for Classification of Breast Lesions. IEICE Transactions on Information and Systems, 2016, E99.D, 1663-1670.	0.7	1
88	Urinary bladder segmentation in CT urography using deepâ€learning convolutional neural network and level sets. Medical Physics, 2016, 43, 1882-1896.	3.0	192
89	Reference state estimation of breast computed tomography for registration with digital mammography. Proceedings of SPIE, 2016, , .	0.8	0
90	Digital breast tomosynthesis reconstruction using spatially weighted non-convex regularization. Proceedings of SPIE, 2016, , .	0.8	4

#	Article	IF	CITATIONS
91	Deep-learning convolution neural network for computer-aided detection of microcalcifications in digital breast tomosynthesis. Proceedings of SPIE, 2016, , .	0.8	28
92	First and second-order features for detection of masses in digital breast tomosynthesis. Proceedings of SPIE, 2016, , .	0.8	1
93	Comment on "Large area CMOS active pixel sensor xâ€ray imager for digital breast tomosynthesis: Analysis, modeling, and characterization―[Med. Phys. 42 , 6294–6308 (2015)]. Medical Physics, 2016, 43, 1578-1579.	3.0	1
94	Computerized flow and vessel wall analyses of coronary arteries for detection of non-calcified plaques in coronary CT angiography. , 2016, , .		0
95	Comparison of bladder segmentation using deep-learning convolutional neural network with and without level sets. Proceedings of SPIE, 2016, , .	0.8	3
96	Automated identification of best-quality coronary artery segments from multiple-phase coronary CT angiography (cCTA) for vessel analysis. , 2016, , .		0
97	Automatic staging of bladder cancer on CT urography. , 2016, , .		Ο
98	Quantitative Analysis of MR Imaging to Assess Treatment Response for Patients with Multiple Myeloma by Using Dynamic Intensity Entropy Transformation: A Preliminary Study. Radiology, 2016, 278, 449-457.	7.3	7
99	Multiscale bilateral filtering for improving image quality in digital breast tomosynthesis. Medical Physics, 2015, 42, 182-195.	3.0	20
100	Computer-aided detection system for clustered microcalcifications in digital breast tomosynthesis using joint information from volumetric and planar projection images. Physics in Medicine and Biology, 2015, 60, 8457-8479.	3.0	28
101	Computer-aided detection of bladder mass within contrast-enhanced region of CTU. , 2015, , .		Ο
102	Robustness evaluation of a computer-aided detection system for pulmonary embolism (PE) in CTPA using independent test set from multiple institutions. Proceedings of SPIE, 2015, , .	0.8	2
103	Ureter segmentation in CT urography (CTU) by COMPASS with multiscale Hessian enhancement. Proceedings of SPIE, 2015, , .	0.8	Ο
104	Quantitative analysis of arterial flow properties for detection of non-calcified plaques in ECG-gated coronary CT angiography. Proceedings of SPIE, 2015, , .	0.8	0
105	Automatic selection of best quality vessels from multiple-phase coronary CT angiography (cCTA). , 2015, , .		1
106	Computer aided detection of surgical retained foreign object for prevention. Medical Physics, 2015, 42, 1213-1222.	3.0	6
107	Treatment Response Assessment for Bladder Cancer on CT Based on Computerized Volume Analysis, World Health Organization Criteria, and RECIST. American Journal of Roentgenology, 2015, 205, 348-352.	2.2	7
108	Comparison of computer-aided detection of clustered microcalcifications in digital mammography and digital breast tomosynthesis. Proceedings of SPIE, 2015, , .	0.8	1

#	Article	IF	CITATIONS
109	Digital breast tomosynthesis: application of 2D digital mammography CAD to detection of microcalcification clusters on planar projection image. , 2015, , .		0
110	Novel Associations between Common Breast Cancer Susceptibility Variants and Risk-Predicting Mammographic Density Measures. Cancer Research, 2015, 75, 2457-2467.	0.9	55
111	Detection of urinary bladder mass in CT urography with SPAN. Medical Physics, 2015, 42, 4271-4284.	3.0	10
112	Response. Radiology, 2015, 275, 619.	7.3	0
113	Digital breast tomosynthesis: computer-aided detection of clustered microcalcifications on planar projection images. Physics in Medicine and Biology, 2014, 59, 7457-7477.	3.0	32
114	Coronary CT angiography (cCTA): automated registration of coronary arterial trees from multiple phases. Physics in Medicine and Biology, 2014, 59, 4661-4680.	3.0	9
115	Comparison of CLASS and ITK-SNAP in segmentation of urinary bladder in CT urography. Proceedings of SPIE, 2014, , .	0.8	0
116	COMPASS-based ureter segmentation in CT urography (CTU). Proceedings of SPIE, 2014, , .	0.8	0
117	Computerized luminal analysis for detection of non-calcified plaques in coronary CT angiography. Proceedings of SPIE, 2014, , .	0.8	0
118	False positive reduction of microcalcification cluster detection in digital breast tomosynthesis. Proceedings of SPIE, 2014, , .	0.8	3
119	Automated identification of spinal cord and vertebras on sagittal MRI. Proceedings of SPIE, 2014, , .	0.8	0
120	Digital breast tomosynthesis: effects of projection-view distribution on computer-aided detection of microcalcification clusters. Proceedings of SPIE, 2014, , .	0.8	3
121	Segmentation of urinary bladder in CT urography (CTU) using CLASS with enhanced contour conjoint procedure. Proceedings of SPIE, 2014, , .	0.8	0
122	Computerâ€aided detection of clustered microcalcifications in multiscale bilateral filtering regularized reconstructed digital breast tomosynthesis volume. Medical Physics, 2014, 41, 021901.	3.0	25
123	Computerized detection of noncalcified plaques in coronary CT angiography: Evaluation of topological soft gradient prescreening method and luminal analysis. Medical Physics, 2014, 41, 081901.	3.0	23
124	Multichannel response analysis on 2D projection views for detection of clustered microcalcifications in digital breast tomosynthesis. Medical Physics, 2014, 41, 041913.	3.0	17
125	Digital Breast Tomosynthesis: Observer Performance of Clustered Microcalcification Detection on Breast Phantom Images Acquired with an Experimental System Using Variable Scan Angles, Angular Increments, and Number of Projection Views. Radiology, 2014, 273, 675-685.	7.3	47
126	Computerized analysis of coronary artery disease: Performance evaluation of segmentation and tracking of coronary arteries in CT angiograms. Medical Physics, 2014, 41, 081912.	3.0	12

#	Article	IF	CITATIONS
127	Digital breast tomosynthesis: studies of the effects of acquisition geometry on contrast-to-noise ratio and observer preference of low-contrast objects in breast phantom images. Physics in Medicine and Biology, 2014, 59, 5883-5902.	3.0	37
128	Surgical retained foreign object (RFO) prevention by computer aided detection (CAD). Proceedings of SPIE, 2014, , .	0.8	1
129	CT urography: segmentation of urinary bladder using CLASS with local contour refinement. Physics in Medicine and Biology, 2014, 59, 2767-2785.	3.0	15
130	Genome-wide association study identifies multiple loci associated with both mammographic density and breast cancer risk. Nature Communications, 2014, 5, 5303.	12.8	109
131	Ureter tracking and segmentation in CT urography (CTU) using COMPASS. Medical Physics, 2014, 41, 121906.	3.0	2
132	Digital breast tomosynthesis reconstruction with an adaptive voxel grid. , 2014, , .		1
133	A similarity study of contentâ€based image retrieval system for breast cancer using decision tree. Medical Physics, 2013, 40, 012901.	3.0	8
134	087001.	3.0	102
135	Quality assurance and training procedures for computerâ€aided detection and diagnosis systems in	3.0	22
136	Auto-Initialized Cascaded Level Set (AI-CALS) Segmentation of Bladder Lesions on Multidetector Row CT Urography. Academic Radiology, 2013, 20, 148-155.	2.5	31
137	Automatic identification of origins of left and right coronary arteries in CT angiography for coronary arterial tree tracking and plaque detection. Proceedings of SPIE, 2013, , .	0.8	1
138	Detection of microcalcifications in breast tomosynthesis reconstructed with multiscale bilateral filtering regularization. , 2013, , .		4
139	Neural network training by maximization of the area under the ROC curve: application to characterization of masses on breast ultrasound as malignant or benign. Proceedings of SPIE, 2013, , .	0.8	1
140	Computerized detection of non-calcified plaques in coronary CT angiography: topological soft-gradient detection method for plaque prescreening. , 2013, , .		1
141	Multiscale intensity homogeneity transformation method and its application to computer-aided detection of pulmonary embolism in computed tomographic pulmonary angiography (CTPA). Proceedings of SPIE, 2013, , .	0.8	0
142	Automated registration of coronary arterial trees from multiple phases in coronary CT angiography (cCTA). Proceedings of SPIE, 2013, , .	0.8	3
143	Curved planar reformation and optimal path tracing (CROP) method for false positive reduction in computer-aided detection of pulmonary embolism in CTPA. , 2013, , .		0
144	Study of image quality in digital breast tomosynthesis by subpixel reconstruction. , 2013, , .		2

#	Article	IF	CITATIONS
145	Computerized segmentation of ureters in CT urography (CTU) using COMPASS. , 2013, , .		1
146	Urinary bladder segmentation in CT urography (CTU) using CLASS. Medical Physics, 2013, 40, 111906.	3.0	12
147	A diffusion-based truncated projection artifact reduction method for iterative digital breast tomosynthesis reconstruction. Physics in Medicine and Biology, 2013, 58, 569-587.	3.0	15
148	Automated iterative neutrosophic lung segmentation for image analysis in thoracic computed tomography. Medical Physics, 2013, 40, 081912.	3.0	36
149	Aromatase inhibitor-induced modulation of breast density: clinical and genetic effects. British Journal of Cancer, 2013, 109, 2331-2339.	6.4	25
150	Breast Mass Characterization Using 3â€Ðimensional Automated Ultrasound as an Adjunct to Digital Breast Tomosynthesis. Journal of Ultrasound in Medicine, 2013, 32, 93-104.	1.7	22
151	Automatic seed point identification and main artery segmentation for pulmonary vascular tree segmentation and tracking in computed tomographic pulmonary angiography (CTPA). Proceedings of SPIE, 2012, , .	0.8	0
152	Segmentation of urinary bladder in CT urography. , 2012, 2012, 3978-81.		0
153	Computer-aided detection of microcalcifications in digital breast tomosynthesis (DBT): a multichannel signal detection approach on projection views. Proceedings of SPIE, 2012, , .	0.8	1
154	Segmentation of urinary bladder in CT urography (CTU) using CLASS. Proceedings of SPIE, 2012, , .	0.8	4
155	A similarity study between the query mass and retrieved masses using decision tree content-based image retrieval (DTCBIR) CADx system for characterization of ultrasound breast mass images. Proceedings of SPIE, 2012, , .	0.8	1
156	Interactive content-based image retrieval (CBIR) computer-aided diagnosis (CADx) system for ultrasound breast masses using relevance feedback. , 2012, , .		3
157	Pulmonary vessel segmentation utilizing curved planar reformation and optimal path finding (CROP) in computed tomographic pulmonary angiography (CTPA) for CAD applications. Proceedings of SPIE, 2012, , .	0.8	7
158	Digital Breast Tomosynthesis Is Comparable to Mammographic Spot Views for Mass Characterization. Radiology, 2012, 262, 61-68.	7.3	142
159	Multiscale regularized reconstruction for enhancing microcalcification in digital breast tomosynthesis. Proceedings of SPIE, 2012, , .	0.8	6
160	Automated coronary artery tree extraction in coronary CT angiography using a multiscale enhancement and dynamic balloon tracking (MSCAR-DBT) method. Computerized Medical Imaging and Graphics, 2012, 36, 1-10.	5.8	48
161	Inter- and Intra-Observer Variability of Radiologists Evaluating CBIR Systems. Lecture Notes in Computer Science, 2012, , 482-489.	1.3	3
162	Improving Image Quality of Digital Breast Tomosynthesis by Artifact Reduction. Lecture Notes in Computer Science, 2012, , 745-752.	1.3	1

#	Article	IF	CITATIONS
163	Breast Parenchymal Pattern (BPP) Analysis: Comparison of Digital Mammograms and Breast Tomosynthesis. Lecture Notes in Computer Science, 2012, , 514-520.	1.3	Ο
164	TH-E-217BCD-10: The Effect of Model Based Iterative Reconstruction (GE-VEO) on the CT Numbers and Noise of Both Small Lung Nodules and Large Homogeneous (heart and Spongiosa) Regions in an Anthropomorphic Chest Phantom. Medical Physics, 2012, 39, 4016-4016.	3.0	0
165	BI-RADS guided mammographic mass retrieval. Proceedings of SPIE, 2011, , .	0.8	4
166	Computerâ€aided detection of breast masses: Fourâ€view strategy for screening mammography. Medical Physics, 2011, 38, 1867-1876.	3.0	25
167	Similarity evaluation between query and retrieved masses using a content-based image retrieval (CBIR) CADx system for characterization of breast masses on ultrasound images: an observer study. Proceedings of SPIE, 2011, , .	0.8	0
168	Study of adaptability of breast density analysis system developed for screen film mammograms (SFMs) to full-field digital mammograms (FFDMs): robustness of parenchymal texture analysis. , 2011, , .		0
169	Computerized detection of pulmonary embolism in computed tomographic pulmonary angiography (CTPA): improvement of vessel segmentation. Proceedings of SPIE, 2011, , .	0.8	0
170	Computer-aided detection of breast masses in digital breast tomosynthesis (DBT): improvement of false positive reduction by optimization of object segmentation. Proceedings of SPIE, 2011, , .	0.8	6
171	Analysis of the number of distinct findings obtained by multiple readers in an MRMC study: When do findings obtained from the addition of new readers become redundant, or otherwise negligible?. , 2011, , .		Ο
172	Image quality of microcalcifications in digital breast tomosynthesis: Effects of projection-view distributions. Medical Physics, 2011, 38, 5703-5712.	3.0	33
173	Computer-aided detection of clustered microcalcifications in digital breast tomosynthesis: A 3D approach. Medical Physics, 2011, 39, 28-39.	3.0	49
174	Similarity evaluation in a contentâ€based image retrieval (CBIR) CADx system for characterization of breast masses on ultrasound images. Medical Physics, 2011, 38, 1820-1831.	3.0	24
175	Adaptive diffusion regularization for enhancement of microcalcifications in digital breast tomosynthesis (DBT) reconstruction. Proceedings of SPIE, 2011, , .	0.8	7
176	Association of Computerized Mammographic Parenchymal Pattern Measure with Breast Cancer Risk: A Pilot Case-Control Study. Radiology, 2011, 260, 42-49.	7.3	75
177	Dynamic multiple thresholding breast boundary detection algorithm for mammograms. Medical Physics, 2010, 37, 391-401.	3.0	16
178	Digital breast tomosynthesis: computerized detection of microcalcifications in reconstructed breast volume using a 3D approach. Proceedings of SPIE, 2010, , .	0.8	1
179	Interobserver variability effects on computerized volume analysis of treatment response of head and neck lesions in CT. , 2010, , .		0
180	Digital breast tomosynthesis: feasibility of automated detection of microcalcification clusters on projections views. , 2010, , .		1

#	Article	IF	CITATIONS
181	Computerized image analysis: Textureâ€field orientation method for pectoral muscle identification on MLOâ€view mammograms. Medical Physics, 2010, 37, 2289-2299.	3.0	16
182	Characterization of masses in digital breast tomosynthesis: Comparison of machine learning in projection views and reconstructed slices. Medical Physics, 2010, 37, 3576-3586.	3.0	28
183	Effect of finite sample size on feature selection and classification: A simulation study. Medical Physics, 2010, 37, 907-920.	3.0	53
184	Selectiveâ€diffusion regularization for enhancement of microcalcifications in digital breast tomosynthesis reconstruction. Medical Physics, 2010, 37, 6003-6014.	3.0	35
185	Association of a mammographic parenchymal pattern (MPP) descriptor with breast cancer risk: a case-control study. , 2010, , .		1
186	Automated segmentation and tracking of coronary arteries in cardiac CT scans: comparison of performance with a clinically used commercial software. Proceedings of SPIE, 2010, , .	0.8	2
187	Effects of projection-view distributions on image quality of calcifications in digital breast tomosynthesis (DBT) reconstruction. Proceedings of SPIE, 2010, , .	0.8	2
188	Treatment Response Assessment of Head and Neck Cancers on CT Using Computerized Volume Analysis. American Journal of Neuroradiology, 2010, 31, 1744-1751.	2.4	16
189	Head and Neck Cancers on CT: Preliminary Study of Treatment Response Assessment Based on Computerized Volume Analysis. American Journal of Roentgenology, 2010, 194, 1083-1089.	2.2	13
190	Computer-Aided Diagnosis of Lung Nodules on CT Scans:. Academic Radiology, 2010, 17, 323-332.	2.5	39
191	Quantitative CT of lung nodules: Dependence of calibration on patient body size, anatomic region, and calibration nodule size for single- and dual-energy techniques. Medical Physics, 2009, 36, 3107-3121.	3.0	11
192	A new automated method for the segmentation and characterization of breast masses on ultrasound images. Medical Physics, 2009, 36, 1553-1565.	3.0	34
193	Computerâ€aided diagnosis of pulmonary nodules on CT scans: Improvement of classification performance with nodule surface features. Medical Physics, 2009, 36, 3086-3098.	3.0	128
194	Multi-modality CADx. Academic Radiology, 2009, 16, 810-818.	2.5	29
195	Effect of CAD on Radiologists' Detection of Lung Nodules on Thoracic CT Scans: Analysis of an Observer Performance Study by Nodule Size. Academic Radiology, 2009, 16, 1518-1530.	2.5	107
196	Evaluation of computerized detection of pulmonary embolism in independent data sets of computed tomographic pulmonary angiographic (CTPA) scans. , 2009, , .		0
197	Artifact Reduction Methods for Truncated Projections in Iterative Breast Tomosynthesis Reconstruction. Journal of Computer Assisted Tomography, 2009, 33, 426-435.	0.9	27
198	Comparison of breast parenchymal pattern on prior mammograms of breast cancer patients and normal subjects. Proceedings of SPIE, 2009, , .	0.8	0

#	Article	IF	CITATIONS
199	Automated segmentation of urinary bladder and detection of bladder lesions in multi-detector row CT urography. , 2009, , .		5
200	Computerâ€aided detection of breast masses on mammograms: Dual system approach with twoâ€view analysis. Medical Physics, 2009, 36, 4451-4460.	3.0	45
201	Treatment response assessment of breast masses on dynamic contrastâ€enhanced magnetic resonance scans using fuzzy â€means clustering and level set segmentation. Medical Physics, 2009, 36, 5052-5063.	3.0	22
202	Computer-aided detection of pulmonary embolism in computed tomographic pulmonary angiography (CTPA): Performance evaluation with independent data sets. Medical Physics, 2009, 36, 3385-3396.	3.0	21
203	Inter- and intra-observer variability in radiologists' assessment of mass similarity on mammograms. , 2009, , .		2
204	Comparison of computerized mass detection in digital breast tomosynthesis (DBT) mammograms and conventional mammograms. , 2009, , .		0
205	A computer-aided diagnosis system for prediction of the probability of malignancy of breast masses on ultrasound images. , 2009, , .		3
206	Computer-Aided Diagnosis in Breast Tomosynthesis and Chest CT. Japanese Journal of Radiological Technology, 2009, 65, 968-976.	0.1	4
207	Characterization of mammographic masses based on level set segmentation with new image features and patient information. Medical Physics, 2008, 35, 280-290.	3.0	92
208	Classifier performance estimation under the constraint of a finite sample size: Resampling schemes applied to neural network classifiers. Neural Networks, 2008, 21, 476-483.	5.9	25
209	Performance Analysis of Three-Class Classifiers: Properties of a 3-D ROC Surface and the Normalized Volume Under the Surface for the Ideal Observer. IEEE Transactions on Medical Imaging, 2008, 27, 215-227.	8.9	19
210	Automated detection of breast vascular calcification on full-field digital mammograms. Proceedings of SPIE, 2008, , .	0.8	10
211	Computer-Aided Diagnosis of Lung Cancer and Pulmonary Embolism in Computed Tomography—A Review. Academic Radiology, 2008, 15, 535-555.	2.5	71
212	Breast Mass Classification on Full-Field Digital Mammography and Screen-Film Mammography. Lecture Notes in Computer Science, 2008, , 371-377.	1.3	1
213	Concordance of computer-extracted image features with BI-RADS descriptors for mammographic mass margin. Proceedings of SPIE, 2008, , .	0.8	9
214	Mammographic Breast Density—Evidence for Genetic Correlations with Established Breast Cancer Risk Factors. Cancer Epidemiology Biomarkers and Prevention, 2008, 17, 3509-3516.	2.5	17
215	Computer-aided detection of masses in digital tomosynthesis mammography: Comparison of three approaches. Medical Physics, 2008, 35, 4087-4095.	3.0	81
216	Design and evaluation of a new automated method for the segmentation and characterization of masses on ultrasound images. , 2008, , .		0

#	Article	IF	CITATIONS
217	Volume analysis of treatment response of head and neck lesions using 3D level set segmentation. Proceedings of SPIE, 2008, , .	0.8	0
218	Truncation artifact and boundary artifact reduction in breast tomosynthesis reconstruction. , 2008, , . \cdot		2
219	Digital tomosynthesis mammography: comparison of mass classification using 3D slices and 2D projection views. Proceedings of SPIE, 2008, , .	0.8	1
220	Classification of breast masses and normal tissues in digital tomosynthesis mammography. Proceedings of SPIE, 2008, , .	0.8	0
221	Breast mass segmentation on dynamic contrast-enhanced magnetic resonance scans using the level set method. , 2008, , .		2
222	Comparison of mammographic parenchymal patterns of normal subjects and breast cancer patients. , 2008, , .		6
223	Automated detection of ureteral wall thickening on multi-detector row CT urography. , 2008, , .		1
224	Digital tomosynthesis mammography: improvement of artifact reduction method for high-attenuation objects on reconstructed slices. , 2008, , .		2
225	Automated segmentation and tracking of coronary arteries in ECG-gated cardiac CT scans. Proceedings of SPIE, 2008, , .	0.8	2
226	Effect of CT scanning parameters on volumetric measurements of pulmonary nodules by 3D active contour segmentation: a phantom study. Physics in Medicine and Biology, 2008, 53, 1295-1312.	3.0	52
227	Characterization of posterior acoustic features of breast masses on ultrasound images using artificial neural network. Proceedings of SPIE, 2008, , .	0.8	1
228	Anniversary Paper: History and status of CAD and quantitative image analysis: The role of <i>Medical Physics</i> and AAPM. Medical Physics, 2008, 35, 5799-5820.	3.0	250
229	Classifier performance prediction for computerâ€aided diagnosis using a limited dataset. Medical Physics, 2008, 35, 1559-1570.	3.0	93
230	Automated regional registration and characterization of corresponding microcalcification clusters on temporal pairs of mammograms for interval change analysis. Medical Physics, 2008, 35, 5340-5350.	3.0	13
231	Detection of Masses in Digital Breast Tomosynthesis Mammography: Effects of the Number of Projection Views and Dose. Lecture Notes in Computer Science, 2008, , 279-285.	1.3	7
232	Computerized Detection and Classification of Malignant and Benign Microcalcifications on Full Field Digital Mammograms. Lecture Notes in Computer Science, 2008, , 336-342.	1.3	4
233	Automated Registration of Volumes of Interest for a Combined X-Ray Tomosynthesis and Ultrasound Breast Imaging System. Lecture Notes in Computer Science, 2008, , 463-468.	1.3	6
234	Investigation of Different PV Distributions in Digital Breast Tomosynthesis (DBT) Mammography. Lecture Notes in Computer Science, 2008, , 593-600.	1.3	7

#	Article	IF	CITATIONS
235	Application of boundary detection information in breast tomosynthesis reconstruction. Medical Physics, 2007, 34, 3603-3613.	3.0	25
236	Classifier Performance Estimation Under the Constraint of a Finite Sample Size: Resampling Schemes Applied to Neural Network Classifiers. Neural Networks (IJCNN), International Joint Conference on, 2007, , .	0.0	5
237	Malignant and Benign Breast Masses on 3D US Volumetric Images: Effect of Computer-aided Diagnosis on Radiologist Accuracy. Radiology, 2007, 242, 716-724.	7.3	128
238	Automated volume analysis of head and neck lesions on CT scans using 3D level set segmentation. Medical Physics, 2007, 34, 4399-4408.	3.0	39
239	Computer-aided detection system for clustered microcalcifications: comparison of performance on full-field digital mammograms and digitized screen-film mammograms. Physics in Medicine and Biology, 2007, 52, 981-1000.	3.0	20
240	Computer-aided diagnosis for interval change analysis of lung nodule features in serial CT examinations. , 2007, , .		5
241	A dynamic multiple thresholding method for automated breast boundary detection in digitized mammograms. , 2007, , .		3
242	Investigation of the Z-axis resolution of breast tomosynthesis mammography systems. , 2007, , .		6
243	Pulmonary nodule registration in serial CT scans using rib anatomy and nodule template matching. , 2007, , .		0
244	Computer-aided detection of masses in digital tomosynthesis mammography: combination of 3D and 2D detection information. , 2007, , .		5
245	Computer-aided detection of breast masses on prior mammograms. , 2007, , .		Ο
246	Digital tomosynthesis mammography: intra- and interplane artifact reduction for high-contrast objects on reconstructed slices using a priori 3D geometrical information. , 2007, , .		7
247	Effect of CAD on radiologists' detection of lung nodules on thoracic CT scans: observer performance study. , 2007, , .		15
248	Automated detection of pulmonary embolism (PE) in computed tomographic pulmonary angiographic (CTPA) images: multiscale hierachical expectation-maximization segmentation of vessels and PEs. , 2007, , .		7
249	Pulmonary nodule registration in serial CT scans based on rib anatomy and nodule template matching. Medical Physics, 2007, 34, 1336-1347.	3.0	24
250	Bilateral analysis based false positive reduction for computerâ€∎ided mass detection. Medical Physics, 2007, 34, 3334-3344.	3.0	47
251	The effect of nodule segmentation on the accuracy of computerized lung nodule detection on CT scans: comparison on a data set annotated by multiple radiologists. , 2007, , .		13
252	Quasi-Continuous and Discrete Confidence Rating Scales for Observer Performance Studies. Academic Radiology, 2007, 14, 38-48.	2.5	19

#	Article	IF	CITATIONS
253	Computer-Aided Detection Systems for Breast Masses: Comparison of Performances on Full-Field Digital Mammograms and Digitized Screen-Film Mammograms. Academic Radiology, 2007, 14, 659-669.	2.5	24
254	Automatic multiscale enhancement and segmentation of pulmonary vessels in CT pulmonary angiography images for CAD applications. Medical Physics, 2007, 34, 4567-4577.	3.0	72
255	Computer-aided diagnosis of pulmonary nodules on CT scans: Segmentation and classification using 3D active contours. Medical Physics, 2006, 33, 2323-2337.	3.0	184
256	A comparative study of limited-angle cone-beam reconstruction methods for breast tomosynthesis. Medical Physics, 2006, 33, 3781-3795.	3.0	244
257	Joint two-view information for computerized detection of microcalcifications on mammograms. Medical Physics, 2006, 33, 2574-2585.	3.0	32
258	Computer-aided detection of breast masses on mammograms: bilateral analysis for false positive reduction. , 2006, , .		2
259	Regularized discriminate analysis for breast mass detection on full field digital mammograms. , 2006, ,		1
260	Computer-aided detection of clustered microcalcifications on full-field digital mammograms: A two-view information fusion scheme for FP reduction. , 2006, , .		0
261	Automatic pulmonary vessel segmentation in 3D computed tomographic pulmonary angiographic (CTPA) images. , 2006, , .		6
262	High-speed large-angle mammography tomosynthesis system. , 2006, , .		17
263	Computerized lung nodule detection on screening CT scans: performance on juxta-pleural and internal nodules. , 2006, , .		7
264	Automated detection of ureter abnormalities on multi-detector row CT urography. , 2006, , .		1
265	Advances in computer-aided diagnosis for breast cancer. Current Opinion in Obstetrics and Gynecology, 2006, 18, 64-70.	2.0	50
266	Characterization of corresponding microcalcification clusters on temporal pairs of mammograms for interval change analysis: comparison of classifiers. , 2006, , .		0
267	Performance analysis of 3-class classifiers: properties of the 3D ROC surface and the normalized volume under the surface. , 2006, 6146, 87.		7
268	Tomosynthesis reconstruction using the simultaneous algebraic reconstruction technique (SART) on breast phantom data. , 2006, 6142, 1391.		12
269	Mammographic Density Measured with Quantitative Computer-aided Method: Comparison with Radiologists' Estimates and BI-RADS Categories. Radiology, 2006, 240, 656-665.	7.3	128
270	Breast Masses: Computer-aided Diagnosis with Serial Mammograms. Radiology, 2006, 240, 343-356.	7.3	43

#	Article	IF	CITATIONS
271	Two-view information fusion for improvement of computer-aided detection (CAD) of breast masses on mammograms. , 2006, 6144, 709.		4
272	Dual system approach to computer-aided detection of breast masses on mammograms. Medical Physics, 2006, 33, 4157-4168.	3.0	33
273	Computer aided detection of clusters of microcalcifications on full field digital mammograms. Medical Physics, 2006, 33, 2975-2988.	3.0	72
274	Accuracy of the CT numbers of simulated lung nodules imaged with multi-detector CT scanners. Medical Physics, 2006, 33, 3006-3017.	3.0	36
275	Mammography Tomosynthesis System for High Performance 3D Imaging. Lecture Notes in Computer Science, 2006, , 137-143.	1.3	6
276	Comparison of decision tree classifiers with neural network and linear discriminant analysis classifiers for computer-aided diagnosis: a Monte Carlo simulation study. , 2005, , .		1
277	Computer-aided detection of breast masses on mammograms: performance improvement using a dual system. , 2005, 5747, 9.		1
278	Computerized pectoral muscle identification on MLO-view mammograms for CAD applications. , 2005, , .		4
279	Computer-aided detection of microcalcification clusters on full-field digital mammograms: multiscale pyramid enhancement and false positive reduction using an artificial neural network. , 2005, , .		Ο
280	False-positive reduction using Hessian features in computer-aided detection of pulmonary nodules on thoracic CT images. , 2005, , .		6
281	Effects of the continuous and discrete confidence rating scales in ROC observer studies. , 2005, , .		0
282	Comparison of similarity measures for the task of template matching of masses on serial mammograms. Medical Physics, 2005, 32, 515-529.	3.0	38
283	Computer-aided detection of lung nodules: False positive reduction using a 3D gradient field method and 3D ellipsoid fitting. Medical Physics, 2005, 32, 2443-2454.	3.0	74
284	ROC study of the effect of stereoscopic imaging on assessment of breast lesions. Medical Physics, 2005, 32, 1001-1009.	3.0	20
285	Computer-aided detection of breast masses on full field digital mammograms. Medical Physics, 2005, 32, 2827-2838.	3.0	91
286	Computer-aided Detection System for Breast Masses on Digital Tomosynthesis Mammograms: Preliminary Experience. Radiology, 2005, 237, 1075-1080.	7.3	114
287	Preliminary Investigation of Computer-aided Detection of Pulmonary Embolism in Three-dimensional Computed Tomography Pulmonary Angiography Images1. Academic Radiology, 2005, 12, 782-792.	2.5	55
288	Computer-aided Detection of Breast Cancer. Radiology, 2004, 233, 615-617.	7.3	1

#	Article	IF	CITATIONS
289	Improvement in Radiologists' Characterization of Malignant and Benign Breast Masses on Serial Mammograms with Computer-aided Diagnosis: An ROC Study. Radiology, 2004, 233, 255-265.	7.3	93
290	Sensitivity of Noncommercial Computer-aided Detection System for Mammographic Breast Cancer Detection: Pilot Clinical Trial. Radiology, 2004, 231, 208-214.	7.3	107
291	Computerized nipple identification for multiple image analysis in computer-aided diagnosis. Medical Physics, 2004, 31, 2871-2882.	3.0	36
292	Correlation between mammographic density and volumetric fibroglandular tissue estimated on breast MR images. Medical Physics, 2004, 31, 933-942.	3.0	106
293	An observer study comparing spot imaging regions selected by radiologists and a computer for an automated stereo spot mammography technique. Medical Physics, 2004, 31, 1558-1567.	3.0	1
294	Combination of Digital Mammography with Semi-automated 3D Breast Ultrasound. Technology in Cancer Research and Treatment, 2004, 3, 325-334.	1.9	64
295	Computerized characterization of breast masses on three-dimensional ultrasound volumes. Medical Physics, 2004, 31, 744-754.	3.0	66
296	Assessment methodologies and statistical issues for computer-aided diagnosis of lung nodules in computed tomography. Academic Radiology, 2004, 11, 462-475.	2.5	76
297	On the repeated use of databases for testing incremental improvement of computer-aided detection schemes. Academic Radiology, 2004, 11, 103-105.	2.5	12
298	Sample size and validation issues on the development of CAD systems. International Congress Series, 2004, 1268, 872-877.	0.2	5
299	Computerized multiple image analysis on mammograms: performance improvement of nipple identification for registration of multiple views using texture convergence analyses. , 2004, , .		0
300	Assessment of breast lesions on stereoscopic and monoscopic digital specimen mammograms: an ROC study. , 2004, , .		2
301	ROC study of the effects of computer-aided interval change analysis on radiologists' characterization of breast masses in two-view serial mammograms. , 2004, , .		0
302	Multimodality CAD: combination of computerized classification techniques based on mammograms and 3D ultrasound volumes for improved accuracy in breast mass characterization. , 2004, , .		2
303	Computer-aided detection of breast masses on full-field digital mammograms: false positive reduction using gradient field analysis. , 2004, 5370, 992.		4
304	Computer-aided detection of lung nodules: false positive reduction using a 3D gradient field method. , 2004, , .		9
305	Design of three-class classifiers in computer-aided diagnosis: Monte Carlo simulation study. , 2003, , .		19
306	Computerized detection of pulmonary embolism in 3D computed tomographic (CT) images: vessel tracking and segmentation techniques. , 2003, , .		19

#	Article	IF	CITATIONS
307	Evaluation of the transmitted exposure through lead equivalent aprons used in a radiology department, including the contribution from backscatter. Medical Physics, 2003, 30, 1033-1038.	3.0	101
308	Effects of magnification and zooming on depth perception in digital stereomammography: an observer performance study. Physics in Medicine and Biology, 2003, 48, 3721-3734.	3.0	7
309	Three-dimensional active contour model for characterization of solid breast masses on three-dimensional ultrasound images. , 2003, , .		1
310	Digital indirect-detection x-ray imagers with microlens focusing: effects of Fresnel reflections from the microlens layer. , 2003, , .		1
311	ROC study: effects of computer-aided diagnosis on radiologists' characterization of malignant and benign breast masses in temporal pairs of mammograms. , 2003, 5032, 94.		1
312	Evaluation of light collection in digital indirect detection x-ray imagers: Monte Carlo simulations with a more realistic phosphor screen model. , 2003, , 54-58.		1
313	The effects of stereo shift angle, geometric magnification and display zoom on depth measurements in digital stereomammography. Medical Physics, 2002, 29, 2725-2734.	3.0	12
314	Breast Cancer Detection: Evaluation of a Mass-Detection Algorithm for Computer-aided Diagnosis—Experience in 263 Patients. Radiology, 2002, 224, 217-224.	7.3	75
315	Optimal neural network architecture selection: effects on computer-aided detection of mammographic microcalcifications. , 2002, 4684, 1325.		1
316	Use of joint two-view information for computerized lesion detection on mammograms: improvement of microcalcification detection accuracy. , 2002, 4684, 754.		1
317	Computer-aided characterization of malignant and benign microcalcification clusters based on the analysis of temporal change of mammographic features. , 2002, , .		4
318	<title>Digital stereomammography: observer performance study of the effects of magnification and zooming on depth perception</title> . , 2002, 4682, 163.		2
319	Lung nodule detection on thoracic computed tomography images: Preliminary evaluation of a computer-aided diagnosis system. Medical Physics, 2002, 29, 2552-2558.	3.0	270
320	Improvement of computerized mass detection on mammograms: Fusion of two-view information. Medical Physics, 2002, 29, 238-247.	3.0	109
321	Optimal Neural Network Architecture Selection. Academic Radiology, 2002, 9, 420-429.	2.5	63
322	Analysis of temporal changes of mammographic features: Computer-aided classification of malignant and benign breast masses. Medical Physics, 2001, 28, 2309-2317.	3.0	65
323	Improvement of mammographic mass characterization using spiculation measures and morphological features. Medical Physics, 2001, 28, 1455-1465.	3.0	166
324	Computer-aided characterization of mammographic masses: accuracy of mass segmentation and its effects on characterization. IEEE Transactions on Medical Imaging, 2001, 20, 1275-1284.	8.9	152

#	Article	IF	CITATIONS
325	Analysis of Uncertainties in Estimates of Components of Variance in Multivariate ROC Analysis. Academic Radiology, 2001, 8, 616-622.	2.5	35
326	Digital Mammography. Academic Radiology, 2001, 8, 454-466.	2.5	24
327	<title>Integer wavelet compression guided by a computer-aided detection system in mammography</title> . , 2001, , .		1
328	<title>Computerized lung nodule detection on thoracic CT images: combined rule-based and statistical classifier for false-positive reduction</title> . , 2001, , .		4
329	<title>Analysis of components of variance in multiple-reader studies of computer-aided diagnosis
with different tasks</title> .,2001,,.		2
330	<title>Recognition of lesion correspondence on two mammographic views: a new method of false-positive reduction for computerized mass detection</title> .,2001,,.		8
331	Multiple-reader studies, digital mammography, computer-aided diagnosis, and the Holy Grail of imaging physics: II. , 2001, 4320, 619.		4
332	<title>Analysis of temporal change of mammographic features for computer-aided characterization of malignant and benign masses</title> .,2001,,.		3
333	<title>Improvement of mammographic lesion detection by fusion of information from different views</title> .,2001,,.		6
334	Computerized image analysis: Estimation of breast density on mammograms. Medical Physics, 2001, 28, 1056-1069.	3.0	157
335	Selection of an optimal neural network architecture for computer-aided detection of microcalcifications-Comparison of automated optimization techniques. Medical Physics, 2001, 28, 1937-1948.	3.0	24
336	Automated registration of breast lesions in temporal pairs of mammograms for interval change analysis-local affine transformation for improved localization. Medical Physics, 2001, 28, 1070-1079.	3.0	29
337	<title>Interval change analysis in temporal pairs of mammograms using a local affine
transformation</title> . , 2000, , .		3
338	<title>Evaluation of an automated computer-aided diagnosis system for the detection of masses on prior mammograms</title> . , 2000, 3979, 967.		9
339	Adverse Effects of Increased Body Weight on Quantitative Measures of Mammographic Image Quality. American Journal of Roentgenology, 2000, 175, 805-810.	2.2	31
340	Stereomammography: Evaluation of depth perception using a virtual 3D cursor. Medical Physics, 2000, 27, 1305-1310.	3.0	14
341	Feature selection and classifier performance in computer-aided diagnosis: The effect of finite sample size. Medical Physics, 2000, 27, 1509-1522.	3.0	112
342	Phototimer setup for CR imaging. Medical Physics, 2000, 27, 2652-2658.	3.0	23

#	Article	IF	CITATIONS
343	Improvement of Radiologists' Characterization of Mammographic Masses by Using Computer-aided Diagnosis: An ROC Study. Radiology, 1999, 212, 817-827.	7.3	262
344	A regional registration technique for automated interval change analysis of breast lesions on mammograms. Medical Physics, 1999, 26, 2669-2679.	3.0	41
345	Combined adaptive enhancement and region-growing segmentation of breast masses on digitized mammograms. Medical Physics, 1999, 26, 1642-1654.	3.0	95
346	Design and evaluation of an external filter technique for exposure equalization in mammography. Medical Physics, 1999, 26, 1655-1669.	3.0	5
347	Classification of malignant and benign masses based on hybrid ART2LDA approach. IEEE Transactions on Medical Imaging, 1999, 18, 1178-1187.	8.9	62
348	Classifier design for computer-aided diagnosis: Effects of finite sample size on the mean performance of classical and neural network classifiers. Medical Physics, 1999, 26, 2654-2668.	3.0	135
349	<title>Components of variance in ROC analysis of CADx classifier performance: II. Applications of the bootstrap</title> . , 1999, 3661, 523.		3
350	<title>Hybrid unsupervised-supervised approach for computerized classification of malignant and benign masses on mammograms</title> . , 1999, , .		1
351	Classification of compressed breast shapes for the design of equalization filters in x-ray mammography. Medical Physics, 1998, 25, 937-948.	3.0	33
352	Computerized characterization of masses on mammograms: The rubber band straightening transform and texture analysis. Medical Physics, 1998, 25, 516-526.	3.0	179
353	<title>Computerized characterization of breast masses using three-dimensional ultrasound images</title> . , 1998, , .		11
354	Computerized analysis of mammographic microcalcifications in morphological and texture feature spaces. Medical Physics, 1998, 25, 2007-2019.	3.0	184
355	Design of a high-sensitivity classifier based on a genetic algorithm: application to computer-aided diagnosis. Physics in Medicine and Biology, 1998, 43, 2853-2871.	3.0	49
356	<title>Effects of sample size on classifier design for computer-aided diagnosis</title> . , 1998, , .		4
357	Technique to improve the effective fill factor of digital mammographic imagers. , 1998, , .		1
358	<title>Regional mammogram registration technique for automated analysis of interval changes of breast lesions</title> . , 1998, 3338, 118.		6
359	<title>Components of variance in ROC analysis of CADx classifier performance</title> . , 1998, 3338, 859.		7
360	False-positive reduction technique for detection of masses on digital mammograms: Global and local multiresolution texture analysis. Medical Physics, 1997, 24, 903-914.	3.0	52

#	Article	IF	CITATIONS
361	Investigation of the line-pair pattern method for evaluating mammographic focal spot performance. Medical Physics, 1997, 24, 11-15.	3.0	8
362	<title>Characterization of masses on mammograms: significance of using the rubber band straightening transform</title> . , 1997, , .		3
363	<title>Effects of sample size on classifier design: quadratic and neural network classifiers</title> . , 1997, , .		7
364	<title>Finite-sample effects and resampling plans: applications to linear classifiers in computer-aided diagnosis</title> . , 1997, 3034, 467.		20
365	Computerized classification of malignant and benign microcalcifications on mammograms: texture analysis using an artificial neural network. Physics in Medicine and Biology, 1997, 42, 549-567.	3.0	125
366	<title>Unitary ranking in the automated detection of mammographic masses</title> ., 1997, , .		0
367	An adaptive density-weighted contrast enhancement filter for mammographic breast mass detection. IEEE Transactions on Medical Imaging, 1996, 15, 59-67.	8.9	172
368	Classification of mass and normal breast tissue: a convolution neural network classifier with spatial domain and texture images. IEEE Transactions on Medical Imaging, 1996, 15, 598-610.	8.9	363
369	<title>Effects of pixel size on classification of microcalcifications on digitized mammograms</title> . , 1996, , .		5
370	Image compression in digital mammography: Effects on computerized detection of subtle microcalcifications. Medical Physics, 1996, 23, 1325-1336.	3.0	29
371	Automated detection of breast masses on mammograms using adaptive contrast enhancement and texture classification. Medical Physics, 1996, 23, 1685-1696.	3.0	103
372	Image feature selection by a genetic algorithm: Application to classification of mass and normal breast tissue. Medical Physics, 1996, 23, 1671-1684.	3.0	115
373	<title>Classification of masses on mammograms using rubber-band straightening transform and feature analysis</title> . , 1996, 2710, 44.		10
374	<title>Image classification using artifical neural networks</title> ., 1995, , .		5
375	<title>Computerized detection and classification of microcalcifications on mammograms</title> . , 1995, , .		7
376	<title>Automated detection of breast masses on digital mammograms using adaptive density-weighted contrast-enhancement filtering</title> . , 1995, , .		7
377	Artificial convolution neural network for medical image pattern recognition. Neural Networks, 1995, 8, 1201-1214.	5.9	250
378	Computer-aided detection of mammographic microcalcifications: Pattern recognition with an artificial neural network. Medical Physics, 1995, 22, 1555-1567.	3.0	180

#	Article	IF	CITATIONS
379	Classification of mass and normal breast tissue on digital mammograms: Multiresolution texture analysis. Medical Physics, 1995, 22, 1501-1513.	3.0	98
380	Computer-aided classification of mammographic masses and normal tissue: linear discriminant analysis in texture feature space. Physics in Medicine and Biology, 1995, 40, 857-876.	3.0	203
381	<title>Multiresolution texture analysis for classification of mass and normal breast tissue on digital mammograms</title> . , 1995, , .		6
382	Computer-aided diagnosis in mammography: classification of mass and normal tissue by texture analysis. Physics in Medicine and Biology, 1994, 39, 2273-2288.	3.0	54
383	Digitization requirements in mammography: Effects on computer-aided detection of microcalcifications. Medical Physics, 1994, 21, 1203-1211.	3.0	67
384	Automated segmentation of regions of interest on hand radiographs. Medical Physics, 1994, 21, 1293-1300.	3.0	17
385	The Estimation of Occupational Effective Dose in Diagnostic Radiology With Two Dosimeters. Health Physics, 1994, 67, 611-615.	0.5	85
386	Evaluation of a Parallel Hole Grid for Bedside Chest Imaging. Investigative Radiology, 1994, 29, 682-688.	6.2	1
387	Computer-aided diagnosis: Detection and characterization of hyperparathyroidism in digital hand radiographs. Medical Physics, 1993, 20, 983-992.	3.0	6
388	Dynamic Digital Subtraction Evaluation of Regional Pulmonary Ventilation with Nonradioactive Xenon. Investigative Radiology, 1990, 25, 728-734.	6.2	17
389	Improvement in Radiologists?? Detection of Clustered Microcalcifications on Mammograms. Investigative Radiology, 1990, 25, 1102-1110.	6.2	323
390	Computer-aided diagnosis in chest radiology. Journal of Thoracic Imaging, 1990, 5, 67-76.	1.5	56
391	Automated Tracking and Computer Reproduction of Vessels in DSA Images. Investigative Radiology, 1990, 25, 1069-1075.	6.2	23
392	Effects of x-ray beam equalization on mammographic imaging. Medical Physics, 1990, 17, 242-249.	3.0	22
393	Studies of performance of antiscatter grids in digital radiography: Effect on signal-to-noise ratio. Medical Physics, 1990, 17, 655-664.	3.0	50
394	Contrast enhancement of noisy images by windowing: Limitations due to the finite dynamic range of the display system. Medical Physics, 1989, 16, 170-178.	3.0	5
395	Exposure Equalization Technique in Mammography. Investigative Radiology, 1989, 24, 154-157.	6.2	11
396	Optical image processing with liquid-crystal display for image intensifier/television systems. Medical Physics, 1988, 15, 838-845.	3.0	2

#	Article	IF	CITATIONS
397	Digital Characterization Of Clinical Mammographic Microcalcifications: Applications In Computer-Aided Detection. , 1988, 0914, 591.		5
398	Three-Dimensional Reproduction Of Coronary Vascular Trees Using The Double-Square-Box Method Of Tracking. , 1988, , .		8
399	Image feature analysis and computer-aided diagnosis in digital radiography. I. Automated detection of microcalcifications in mammography. Medical Physics, 1987, 14, 538-548.	3.0	280
400	Digital Mammography. Investigative Radiology, 1987, 22, 581-589.	6.2	136
401	<title>Digital Mammography: Development Of A Computer-Aided System For Detection Of
Microcalcifications</title> . Proceedings of SPIE, 1987, 0767, 367.	0.8	2
402	Basic Imaging Properties of a Large Image Intensifier-TV Digital Chest Radiographic System. Investigative Radiology, 1987, 22, 328-335.	6.2	31
403	Automated Tracking Of The Vascular Tree In DSA Images Using A Double-Square-Box Region-Of-Search Algorithm. , 1986, 0626, 326.		27
404	Evaluation Of Digital Unsharp-Mask Filtering For The Detection Of Subtle Mammographic Microcalcifications. Proceedings of SPIE, 1986, 0626, 347.	0.8	1
405	Investigation of basic imaging properties in digital radiography. 8. Detection of simulated low-contrast objects in digital subtraction angiographic images. Medical Physics, 1986, 13, 304-311.	3.0	22
406	Some properties of photon scattering in water phantoms in diagnostic radiology. Medical Physics, 1986, 13, 824-830.	3.0	16
407	Investigation of basic imaging properties in digital radiography. 5. Characteristic curves of II-TV digital systems. Medical Physics, 1986, 13, 13-18.	3.0	28
408	Digital Image Processing: Optimal Spatial Filter For Maximization Of The Perceived Snr Based On A Statistical Decision Theory Model For The Human Observer. Proceedings of SPIE, 1985, 0535, 2.	0.8	7
409	Physical characteristics of scattered radiation in diagnostic radiology: Monte Carlo simulation studies. Medical Physics, 1985, 12, 152-165.	3.0	83
410	Performance of antiscatter grids in diagnostic radiology: Experimental measurements and Monte Carlo simulation studies. Medical Physics, 1985, 12, 449-454.	3.0	37
411	Studies of x-ray energy absorption and quantum noise properties of x-ray screens by use of Monte Carlo simulation. Medical Physics, 1984, 11, 37-46.	3.0	48
412	Radiation dose in diagnostic radiology: Monte Carlo simulation studies. Medical Physics, 1984, 11, 480-490.	3.0	20
413	Experimental and theoretical energy and angular dependencies of scattered radiation in the mammography energy range. Medical Physics, 1983, 10, 664-668.	3.0	16
414	Energy and angular dependence of x-ray absorption and its effect on radiographic response in screen-film systems. Physics in Medicine and Biology, 1983, 28, 565-579.	3.0	72

#	Article	IF	CITATIONS
415	<title>An Empirical Investigation Of Variability In Contrast-Detail Diagram
Measurements</title> . Proceedings of SPIE, 1983, 0419, 68.	0.8	25
416	Investigation of the performance of antiscatter grids: Monte Carlo simulation studies. Physics in Medicine and Biology, 1982, 27, 785-803.	3.0	61
417	Physical characteristics of scattered radiation and the performance of antiscatter grids in diagnostic radiology. Radiographics, 1982, 2, 378-406.	3.3	11
418	Monte Carlo simulation studies of detectors used in the measurement of diagnostic x-ray spectra. Medical Physics, 1980, 7, 627-635.	3.0	43
419	Determination of radiographic screen-film system characteristic curve and its gradient by use of a curve-smoothing technique. Medical Physics, 1978, 5, 443-447.	3.0	8
420	Utilization Of Digital Image Data For Computer-aided Diagnosis. , 0, , .		2
421	Neural network based segmentation using a priori image models. , O, , .		5
422	Neural network design for optimization of the partial area under the receiver operating characteristic curve. , 0, , .		1
423	Automated Registration and Classification Techniques for Interval Change Analysis in Mammography. , 0, , .		1